Spin-polaron effective magnetic model for $La_{0.5}Ca_{0.5}MnO_3$

N. P. Konstantinidis*
Department of Physics and Department of Mathematics, University of Dublin, Trinity College, Dublin 2, Ireland

C. H. Patterson
Department of Physics and Centre for Scientific Computation, University of Dublin, Trinity College, Dublin 2, Ireland
(Received 9 November 2003; revised manuscript received 22 April 2004; published 10 August 2004)

The conventional paradigm of charge order for $La_{1-x}Ca_xMnO_3$ for $x=0.5$ has been challenged recently by a Zener polaron picture emerging from experiments and theoretical calculations. The effective low energy Hamiltonian for the magnetic degrees of freedom has been found to be a cubic Heisenberg model, with ferromagnetic nearest neighbor and frustrating antiferromagnetic next nearest neighbor interactions in the planes, and antiferromagnetic interaction between planes. With linear spin wave theory and diagonalization of small clusters up to 27 sites we find that the behavior of the model interpolates between the A- and CE-type magnetic structures when a frustrating intraplanar interaction is tuned. The values of the interactions calculated by *ab initio* methods indicate a possible non-bipartite picture of polaron ordering differing from the conventional one.

DOI: 10.1103/PhysRevB.70.064407 PACS number(s): 75.47.Lx, 75.10.Jm, 75.30.Ds, 75.50.Ee

I. INTRODUCTION

Charge, orbital and spin order in doped manganites ($A_{1-x}B_xMnO_3$, where A is a trivalent ion and B a divalent ion) with $x \geqslant 0.4$ is generally discussed in terms of the Goodenough model[1] and the double exchange Hamiltonian.[2] In that picture, charge ordering (CO) and orbital ordering (OO) is associated with $3d$ populations of Mn ions, which may be d^3 or d^4. In $La_{0.5}Ca_{0.5}MnO_3$, for example, it is believed that there are equal numbers of Mn ions with d^3 and d^4 populations in the CO state.[3] However, recent experimental and theoretical investigations point to a more complex picture, and there is evidence that a Zener polaron or similar model, which is quite distinct from the original Goodenough model, describes the CO state of $La_{0.5}Ca_{0.5}MnO_3$ and $Pr_{0.60}Ca_{0.40}MnO_3$.[4–6] Here a frustrated Heisenberg Hamiltonian is used to model the Zener polaron state of half-doped manganites using spin wave theory and exact diagonalization of clusters with periodic boundary conditions. The parameter space for the Hamiltonian is derived from *ab initio* calculations on the Zener polaron state of $La_{0.5}Ca_{0.5}MnO_3$.[5] In particular, we report energetics, spin waves, magnetization, spin correlation functions, the spin contribution to heat capacity and magnetic susceptibility for this model.

In the Zener polaron picture pairs of Mn ions are tightly bound into ferromagnetic (FM) dimers which interact relatively weakly with each other.[4,5] The Mn ion $3d$ population is d^4 on all Mn ions and electrons are transferred from O^{2-} ions located between Mn ions in dimers, to form Mn-O^--Mn polarons. Electron transfer is necessary to satisfy electron counting. The dimers (Zener polarons) have spin 7/2. Their electronic structure is reflected in the *Pm* crystal structure of $Pr_{0.60}Ca_{0.40}MnO_3$ determined by neutron scattering from a single crystal.[4] The $P2_1/m$ structure for $La_{0.5}Ca_{0.5}MnO_3$ determined by neutron scattering[3] from a powder is different in several respects. The crystal structure of $La_{0.5}Ca_{0.5}MnO_3$ has been calculated by using *ab initio* methods to minimize the crystal total energy[7] and the resulting structure resembles that for $Pr_{0.60}Ca_{0.40}MnO_3$.[4] The Zener polaron picture for half-doped manganites may therefore apply more generally.[8] In the frustrated Heisenberg Hamiltonian used in this work, polarons are treated as single magnetic units with spin 7/2. This is appropriate for Mn ions tightly bound into FM dimers when the internal FM coupling greatly exceeds the interpolaron coupling. *Ab initio* calculations on $La_{0.5}Ca_{0.5}MnO_3$ show that magnetic coupling within polarons is strong and ferromagnetic ($J \sim 200$ meV), while coupling between polarons along their zig-zag chains is also FM but much weaker ($J \sim 10$ meV).[5] There are both antiferromagnetic (AF) and FM couplings of the same order of magnitude between polarons in neighboring chains so that interchain coupling is strongly frustrated.

Zener polarons and exchange couplings in $La_{0.5}Ca_{0.5}MnO_3$ are shown schematically in Fig. 1, together with the magnetic unit cell. Intrachain FM coupling is labeled FM1. Competing AF and FM intraplanar, interchain couplings are labeled AF1 and FM2; there is also an AF interplanar coupling, AF2, which is not shown. *Ab initio* calculations on $LaMnO_3$ show that exchange coupling constants in that compound depend on OO and that not only the magnitudes, but also the signs of exchange constants can change when OO changes.[9] In both $LaMnO_3$ and $La_{0.5}Ca_{0.5}MnO_3$, AF couplings are found between neighboring Mn ions when their filled e_g orbitals are both oriented perpendicular to a Mn-O-Mn axis, while FM couplings are found between Mn ions when their filled e_g orbitals are oriented perpendicular to each other, one being oriented along the Mn-O-Mn axis and the other perpendicular to it. FM exchange constants FM1 and FM2 in $La_{0.5}Ca_{0.5}MnO_3$ were found to be similar in magnitude by *ab initio* calculation (−12 and −14 meV, respectively);[5] they are assumed to have the same value, J_1, in this work. AF1 and AF2 exchange constants were found to be 5 and 8 meV, respectively, and correspond to J_2 and J_3 in the model described below. It is noted that unrestricted Hartree-Fock (UHF) calculations used to obtain these ex-

 ©2004 The American Physical Society

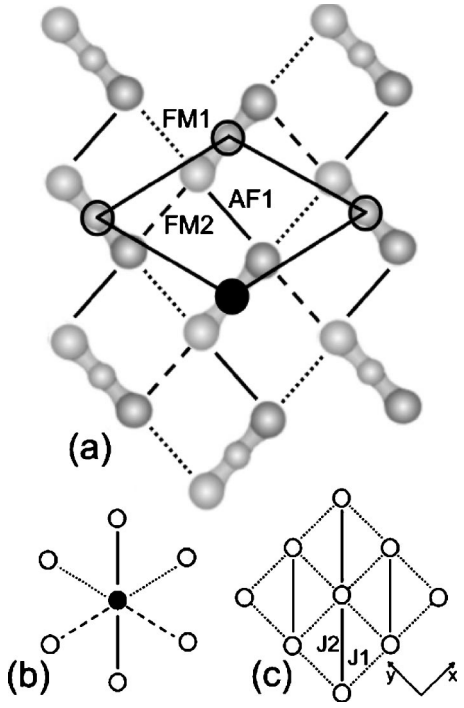

FIG. 1. Schematic illustration of the connectivity of the model: (a) effective exchange interactions between polarons (FM stands for ferromagnetic and AF for antiferromagnetic). (b) Magnetic unit cell. (c) Connectivity of the model in the planes. Interplanar interactions are AF.

change constants underestimate the magnitude of the AF exchange constants in $LaMnO_3$, while the FM exchange constant is in agreement with the experimental value.[9] Inspection of Fig. 1(a) shows that each polaron is ferromagnetically coupled to four neighbors, two on each side, and antiferromagnetically coupled to two neighbors in the same plane [Fig. 1(b)], along the diagonal direction; this arrangement of exchange couplings is equivalent to the model shown in Fig. 1(c).

Half-doped manganites possess either A, CE or C_xE_{1-x} type AF magnetic states below their Néel temperatures, depending on the identities of the ions A and B in $A_{1-x}B_xMnO_3$.[10] CE-type AF order consists of zig-zag FM chains antiferromagnetically coupled to neighboring chains. C_xE_{1-x} order is an incommensurate charge and orbital CE-type order.[11] CE and C_xE_{1-x} order is found for wider gap manganites such as $Pr_{0.60}Ca_{0.40}MnO_3$[4] and $La_{0.5}Ca_{0.5}MnO_3$,[3] while A-type order is found for metallic manganites such as $Pr_{0.5}Ca_{0.5}MnO_3$.[10] Incommensurability and a fine energetic balance between A and CE-type magnetic order are therefore features of the half-doped manganites which also appear in *ab initio* calculations.[5] Magnetic susceptibility data for $Pr_{0.60}Ca_{0.40}MnO_3$ (Ref. 4) has been interpreted in terms of ordering of magnetic moments of Zener polarons in a CE-type state below $T_N = 115$ K, and ordering of magnetic moments into Zener polarons at the CO temperature, $T_{CO} = 330$ K.

The ground state of the classical, magnetic Hamiltonian corresponding to Fig. 1(c) is A-type when the magnitude of J_1 is less than half that of J_2. The ground state changes to an incommensurate spin spiral state with the in-plane component of the wave vector parallel to the diagonal direction of J_2 when the ratio of exchange constants $J_2/|J_1|$ exceeds 0.5. The spin spiral state becomes the commensurate, orthogonal phase described by Efremov *et al.*[6] when the spiral wave vector becomes $(\pi/2, \pi/2, \pi)$; the classical magnetic model predicts that this state is found only in the limit $J_2/|J_1| \to \infty$. Both spin wave theory and cluster diagonalization support a picture in which the magnetic structure in half-doped manganites is strongly dependent on the relative magnitudes of exchange constants J_1 and J_2. Specifically, AF coupling between polarons tunes the magnetic correlations between a state with in-plane ferromagnetism, similar to the A-type structure, and a state where AF correlations are dominant. The latter state is the spin spiral, which is reminiscent of the CE-type structure. A similar picture has emerged in Ref. 6 with non-bipartite magnetic structures competing for the ground state. These authors find that the magnetic structure of the ground state around half-filling is subtly dependent on the extent of doping, x, and for a part of the phase diagram the ground state is intermediate between a conventional CO state and a Zener polaron state.

A two-dimensional Heisenberg model, with frustrated, AF interactions similar to those in the three-dimensional model used here, describes the magnetic properties of organic molecular crystals.[12,13] A Heisenberg model with the same connectivity as that used here has been applied to α'-NaV_2O_2.[14] A similar spin wave approach to the one used in this paper was recently applied to $La_{0.5}Ca_{0.5}MnO_3$.[15] In that work *each* Mn ion was assigned a spin $3/2$ or 2, there were FM couplings within zig-zag chains and AF couplings between spins in adjacent chains. Hence that work differs from the present work in the magnetic units used (single ions versus dimers) and the presence or absence of frustration in interchain coupling.

The plan of the rest of this paper is as follows: in Sec. II the model is introduced and solved at the classical level; in Sec. III linear spin wave theory is applied; in Sec. IV the results of diagonalization of the Hamiltonian for small clusters with periodic boundary conditions are presented. Finally conclusions are presented in Sec. V.

II. HAMILTONIAN AND CLASSICAL SOLUTION

The Heisenberg Hamiltonian used in this work is

$$H = \sum_{i,j,k} [J_1(\mathbf{s}_{i,j,k} \cdot \mathbf{s}_{i+1,j,k} + \mathbf{s}_{i,j,k} \cdot \mathbf{s}_{i,j+1,k}) + J_2 \mathbf{s}_{i,j,k} \cdot \mathbf{s}_{i+1,j+1,k} + J_3 \mathbf{s}_{i,j,k} \cdot \mathbf{s}_{i,j,k+1}]. \quad (1)$$

The FM zig-zag chains are defined by consecutive steps in the $\hat{x}$ and $-\hat{y}$ directions in Fig. 1(c). z is the interplanar axis. i, j and k label sites along the three axes, J_1 is FM and negative while J_2 and J_3 are AF and positive. Interactions within xy planes are frustrated since J_1 prefers parallel spin alignment while J_2 favors antiparallel alignment along the diagonals. The term bond is used to describe these interactions from here on. Ratios of the magnitudes of *ab initio* exchange constants are $J_2/|J_1| = 0.38$ and $J_3/|J_1| = 0.62$ (using

an average value of the FM1 and FM2 of −13 meV for J_1).[5] The interplanar exchange coupling J_3 is not frustrated and the ratio $J_3/|J_1|$ will be fixed at 0.5 from now on, except where noted.

At the classical level,[16,17] the angle between neighboring spins is found by minimizing the structure factor,

$$J(\mathbf{q}) = J_1(\cos q_x + \cos q_y) + J_2 \cos(q_x + q_y) + J_3 \cos q_z. \tag{2}$$

The solution is $\mathbf{q}=(0,0,\pi)$ for $J_2/|J_1| \leqslant 0.5$ and $\mathbf{q}=(q,q,\pi)$ with $q=\arccos(-J_1/2J_2)$ when $J_2/|J_1|>0.5$. The former case corresponds to FM intraplanar order and AF interplanar order; the latter corresponds to a spin spiral in the plane, with the intraplanar component of the wave vector along the direction of the J_2 bond. The angle between neighboring spins is q. In the limit $J_2/|J_1| \to \infty$, $q \to \pi/2$ so that neighboring spins are at right angles; this is the orthogonal phase described in Ref. 6. Thus the solution to Eq. (1) for small $J_2/|J_1|$ corresponds to A-type AF order, while for $J_2/|J_1| \to \infty$ the structure is a noncollinear CE-type magnetic phase.

Clusters of cubic symmetry with $2\times2\times2$ and $3\times3\times3$ sites will be considered in exact diagonalization calculations in Sec. IV. For the second cluster, periodic boundary conditions are frustrated for the AF bonds, due to the odd number of spins along the corresponding directions. For both clusters the classical ground state is FM in the xy plane for $J_2/|J_1| \leqslant 1$, with energies per bond J_1 and J_2. For $J_2/|J_1|>1$, the bond energies are 0 and $-J_2$ for the 8-site cluster, and $J_1/4$ and $-J_2/2$ for the 27-site cluster. For the 8-site cluster this is orthogonal type of magnetic order,[6] while for the 27-site cluster it is a frustrated configuration along the diagonals. Along the z direction the energy per bond is $-J_3$ for 8 sites and $-J_3/2$ for 27, regardless of the value of $J_2/|J_1|$. Frustration in boundary conditions increases the energy for the 27-site cluster. The total energies are $4(2J_1+J_2-J_3)$ for 8 sites and $27(2J_1+J_2-(J_3/2))$ for 27 sites when $J_2/|J_1| \leqslant 1$, and the corresponding energies for $J_2/|J_1|>1$ are $-4(J_2+J_3)$ and $(27/2)(J_1-J_2-J_3)$, respectively. The ratio $J_2/|J_1|$ where the ground state correlations change character is different compared with the infinite lattice value due to the finite size of the clusters.

III. LINEAR SPIN WAVE THEORY

Owing to the spiral nature of the classical ground state for $J_2/|J_1|>0.5$, it is convenient to redefine the s_i operators so that the local quantization axis points along the classical solution spin directions. Only one type of bosonic operator is necessary here, although the Hamiltonian becomes more complex. After introducing the Holstein-Primakoff transformation[18] with operators a and Fourier transforming, the Hamiltonian becomes

$$H = NE_{cl} + S\sum_{\mathbf{k}} \left[A_{\mathbf{k}} a_{\mathbf{k}}^{\dagger} a_{\mathbf{k}} + \frac{B_{\mathbf{k}}}{2}(a_{\mathbf{k}}^{\dagger} a_{-\mathbf{k}}^{\dagger} + a_{\mathbf{k}} a_{-\mathbf{k}}) \right], \tag{3}$$

where N is the number of sites, $E_{cl}=S^2\Sigma_i J_i \cos\theta_i$, $A_{\mathbf{k}}=-\Sigma_i J_i[2\cos\theta_i-(1+\cos\theta_i)\cos(\mathbf{k}\cdot\boldsymbol{\delta}_i)]$ and $B_{\mathbf{k}}=-\Sigma_i J_i(1-\cos\theta_i)\cos(\mathbf{k}\cdot\boldsymbol{\delta}_i)$. i refers to bonds in the unit cell with θ_i the angle at the classical level between two spins connected by bond J_i, and $\boldsymbol{\delta}_i$ the unit vector in the bond's direction. After a Bogoliubov transformation to new operators $\alpha_{\mathbf{k}}$,[19,20] the diagonalized Hamiltonian is

$$H = NE_{cl} + S\left(\sum_{\mathbf{k}} \epsilon_{\mathbf{k}} \alpha_{\mathbf{k}}^{\dagger} \alpha_{\mathbf{k}} + \sum_{\mathbf{k}} \frac{\epsilon_{\mathbf{k}} - A_{\mathbf{k}}}{2} \right), \tag{4}$$

with $\epsilon_{\mathbf{k}}=\sqrt{A_{\mathbf{k}}^2-B_{\mathbf{k}}^2}$. The average spin magnitude per site along the classical solution direction is

$$\langle s_i^z \rangle = s_i + \frac{1}{2} - \frac{1}{2N}\sum_{\mathbf{k}} \frac{A_{\mathbf{k}}}{\epsilon_{\mathbf{k}}}. \tag{5}$$

The ground state energy is found by setting the occupation number $\alpha_{\mathbf{k}}^{\dagger}\alpha_{\mathbf{k}}$ equal to zero for every $\mathbf{k}$. The ground state energy and magnetization per site are plotted in Fig. 2 as a function of $J_2/|J_1|$ with $J_3/|J_1|=0.5$. The correction to the energy for quantum fluctuations for $s_i=7/2$ is very small owing to the large spin magnitude; the classical spin structure survives with only minor changes in the magnetization. The point of maximal frustration where the energy has a maximum is shifted from 0.71 for the classical case to 0.69 in linear spin wave theory. Quantum fluctuations lower the local magnetization from 7/2 per site and there is a minimum in the local magnetic moment when the classical ground state changes from a FM to a spiral state.

Spin wave dispersion relations along (k,k,π) (parallel to the AF J_2 bond), $(k,-k,\pi)$ (perpendicular to the J_2 bond), and $(0,0,k)$ (perpendicular to planes containing zig-zag chains) are shown in Fig. 3. When $J_2/|J_1|=0$, dispersion relations are characteristic of a FM ground state; at the transition point, $J_2/|J_1|=0.5$, the spin wave velocity vanishes along the (k,k,π) direction and magnetization corrections have a local maximum.[21] When $J_2/|J_1|>0.5$, changes in the magnetic ground state to a spin spiral become evident in the dispersion relation along (k,k,π) [Fig. 3(a)]; zero modes appear at the spiraling wave vector, whose magnitude increases with $J_2/|J_1|$. The zero mode occurs at $(\pi/2,\pi/2,\pi)$ when $J_2/|J_1| \to \infty$. When $J_2/|J_1| \leqslant 0.5$, spins are ferromagnetically correlated along the $\hat{x}$ and $\hat{y}$ directions and a dispersion relation characteristic of FM order in the ground state is found [Fig. 3(b)]. But when $J_2/|J_1|>0.5$, a gap develops at $(0,0,\pi)$ since there is a spiral in the planes. AF order from plane to plane along the $(0,0,z)$ direction [Fig. 3(c)] is reduced due to quantum fluctuations as $J_2/|J_1|$ increases, with the energy gain increasing along the J_2 bond. Inclusion of the interplanar interaction makes the system three dimensional and the integrals in the calculation of the ground state energy and the magnetization per site are well-behaved, while in the calculation in Refs. 12 and 21 the planar character of the model enhances the role of quantum fluctuations.[22]

IV. DIAGONALIZATION OF FINITE CLUSTERS

Hamiltonians [Eq. (1)] for three-dimensional clusters with periodic boundary conditions and spin 7/2 or 1/2 were diagonalized after block factorization using permutation and

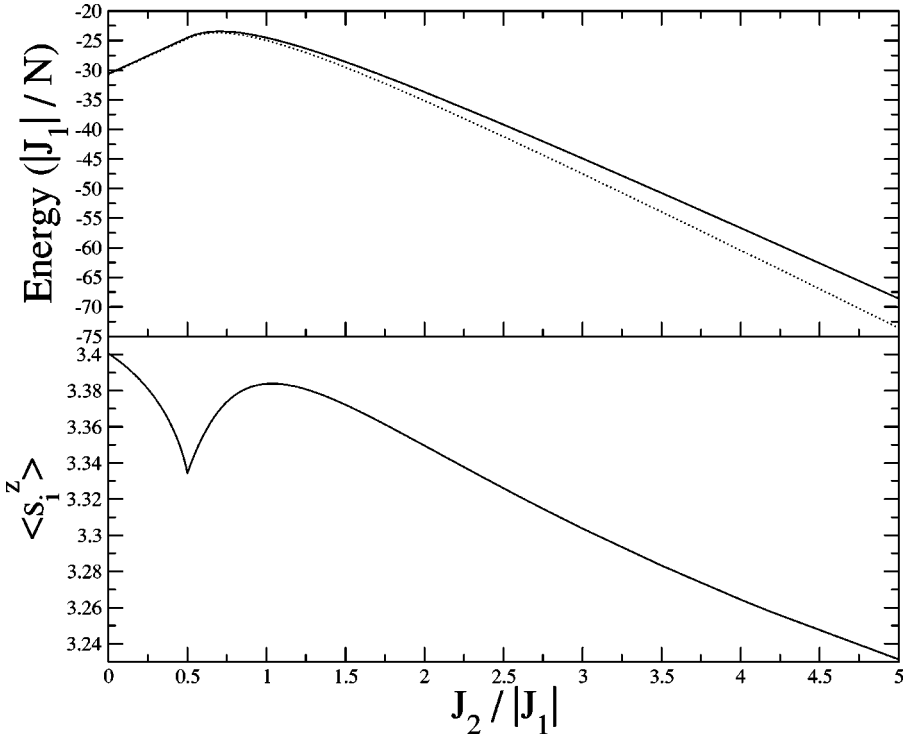

FIG. 2. Ground state energy and magnetization per site as a function of $J_2/|J_1|$ for $J_3/|J_1|=0.5$ within linear spin wave theory. Top: solid line: classical energy, dotted line: spin wave energy.

spin symmetries.[23–25] Hamiltonians for $2\times2\times2$ and $3\times3\times3$ clusters, which have all the symmetries of the bulk, and a $3\times3\times2$ cluster were diagonalized. Energy eigenvalue spectra and nearest and next nearest neighbor correlation functions were computed. Whenever full diagonalization was not possible, lowest eigenvalues were calculated using the numerical package ARPACK.[26,27] The aims were to corroborate results presented above by investigating the influence of quantum fluctuations on the classical results, further study the competition of FM and AF intraplanar and AF interplanar exchange couplings and examine finite-size effects. Diagonalization of Hamiltonians with $s_i=7/2$ was limited to 8-site clusters due to computer memory requirements, whereas Hamiltonians for 27-site clusters could be diagonalized for $s_i=1/2$. The point symmetry group for the cubic clusters is D_{2h}.

The ground state energy for the $2\times2\times2$ $s_i=7/2$ cluster is plotted in Fig. 4(a) for two values of $J_3/|J_1|$ as a function of $J_2/|J_1|$. It is a total spin $S=0$ state with momentum $\mathbf{k}=\mathbf{0}$ and is symmetric with respect to spin inversion. Frustration is maximal for $J_2/|J_1|=0.915\,92$ and $0.918\,95$ when $J_3/|J_1|=0.4$ and 0.5, respectively. The classical transition point

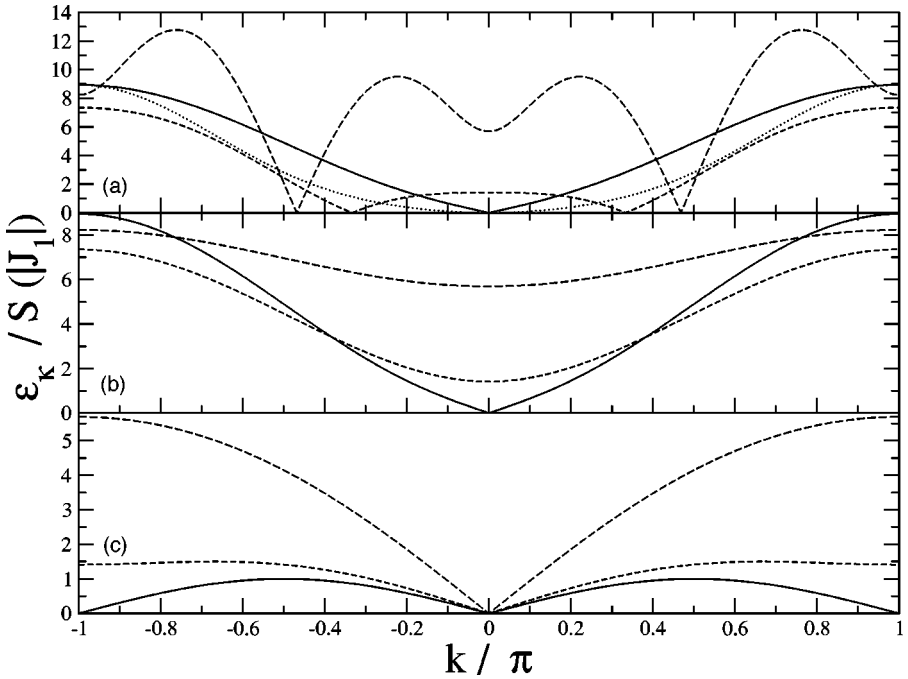

FIG. 3. Dispersion relations along different directions in the Brillouin zone for $J_3/|J_1|=0.5$ within linear spin wave theory. [(a) Top] (k,k,π), [(b) middle] $(k,-k,\pi)$, [(c) bottom] $(0,0,k)$, straight line: $J_2/|J_1|=0$ for top and $0\leqslant J_2/|J_1|\leqslant0.5$ for middle and bottom, dotted line: $J_2/|J_1|=0.5$ for top, dashed line: $J_2/|J_1|=1$, long-dashed line: $J_2/|J_1|=5$.

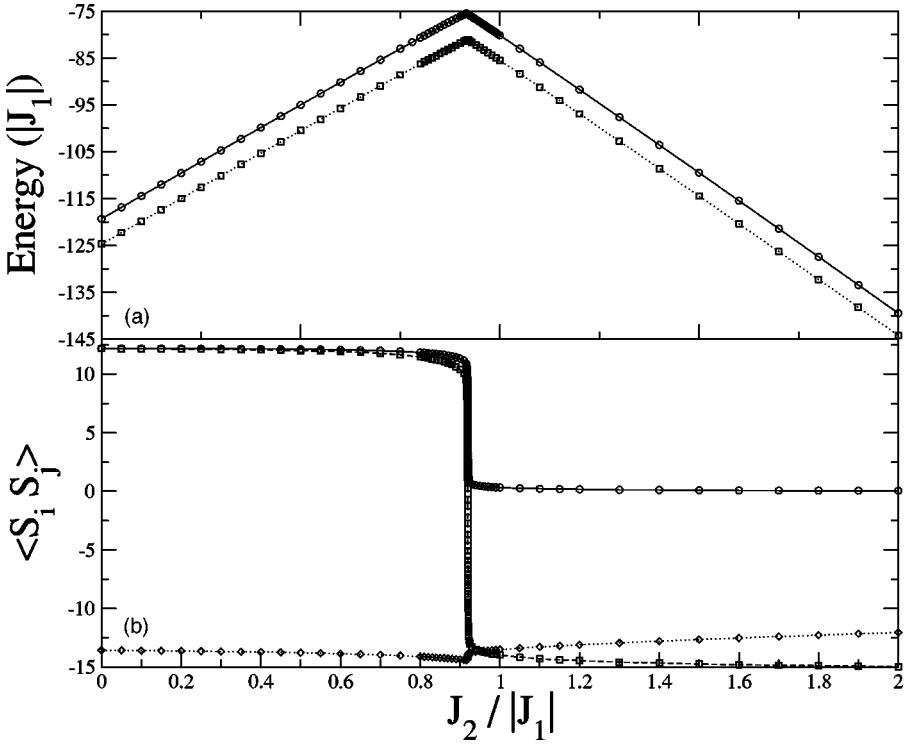

FIG. 4. Energy and nearest and next nearest neighbor correlation functions of the ground state for $s_i = 7/2$ and a $2\times2\times2$ cluster as a function of $J_2/|J_1|$. [(a) Top] $J_3/|J_1| = 0.4$ (○) and $J_3/|J_1| = 0.5$ (□). [(b) Bottom] correlation function for bond J_1 (○), for bond J_2 (□), and for bond J_3 (◇). The lines are guides for the eye.

$J_2/|J_1| = 1$ is therefore renormalized by quantum fluctuations toward smaller $J_2/|J_1|$.

Around the points of maximal frustration the characteristics of the ground state change, as shown by the correlation functions in Fig. 4(b). For small $J_2/|J_1|$ the nearest neighbor and next nearest neighbor correlation functions are strongly FM. For larger $J_2/|J_1|$ the nearest neighbor correlation function is very small, while the next nearest neighbor correlation function becomes strongly AF. At the same time, the interplanar correlation function, which is always AF, loses some of its strength due to quantum fluctuations, with the spins gaining energy predominantly via the AF J_2 bond. The changes in the nature of the correlation functions are quite sharp, similar to the behavior of the energy around maximum frustration. The relative changes of the correlation functions as a function of $J_2/|J_1|$ are very similar to changes in the classical solution. This classical-like behavior is due to the large value of the spin, $s_i = 7/2$.

Calculation of the low energy properties for the 27-site, $s_i = 7/2$ cluster is not possible, as noted above. To study the effect of the frustrating bond J_2 as a function of cluster size, we consider $s_i = 1/2$ and estimate the changes compared to the 8-site case. The ground state energy for $J_3/|J_1| = 0.4$ and 0.5 is shown in Fig. 5(a) for 8 sites. It is an $S = 0$ state with momentum $\mathbf{k} = \mathbf{0}$ and is symmetric with respect to spin inversion. The points of maximal frustration are now around 0.57 and 0.58, respectively, significantly changed from the classical and $s_i = 7/2$ values. The correlation functions are plotted in Fig. 5(b), and the change of the in-plane correlation functions from a FM to a diagonal AF character is now smoother. This is attributed to the smaller magnitude of the spins. The gain in energy via the J_2 bond is now more significant.

For the 27-site cluster the ground state energy for $J_3/|J_1| = 0.4$ and 0.5 is plotted in Fig. 6(a) as a function of $J_2/|J_1|$. Frustration is maximal for $J_2/|J_1| = 0.7212$ and 0.7278. The ground state energy has momentum $\mathbf{k} = (0, 0, \pi)$, which is doubly degenerate. Its point symmetry group is C_{2h}, a subgroup of D_{2h}. The ground state belongs to the A_g irreducible representation.[28] Correlation functions for the ground state are plotted in Fig. 6(b). Their behavior is similar to the correlations in the 8-site cluster and they change character around the point of maximal frustration. The nearest neighbor intraplanar correlation function is 0.247 and almost fully polarized at $J_2/|J_1| = 0$, and then drops to approximately one-third of this value for larger $J_2/|J_1|$. The diagonal correlation function starts with the same strong FM character at $J_2/|J_1| = 0$ and reverses sign for larger values. It is equal to -0.205 for $J_2/|J_1| = 1$, which shows strong AF correlation when compared with the value for $J_1 = 0$, which is -0.238. The interplanar correlation function originally decreases slightly with increasing $J_2/|J_1|$ and for higher values increases slightly to accommodate the increase of the diagonal intraplanar correlation function. Closer inspection of the plot [Fig. 6(b)] reveals two discontinuities in the correlation functions for values of $J_2/|J_1|$ equal to 0.736 341 and 0.750 08, where the two lowest energy states change roles as the ground and the first excited state. The two states have the same momentum and belong to the same irreducible representation, but the ground state between the two discontinuities is an $S = 3/2$ state, while the other is $S = 1/2$. At the same points the derivative of the energy with respect to $J_2/|J_1|$ is discontinuous.

As was the case for the 8-site cluster, the transition from a FM to a spin spiral state has been renormalized by quantum fluctuations, however the corresponding $J_2/|J_1|$ value is closer to the classical value of 1 compared with the 8-site cluster. The changes of the intraplanar correlation functions as functions of $J_2/|J_1|$ are sharper compared with the changes

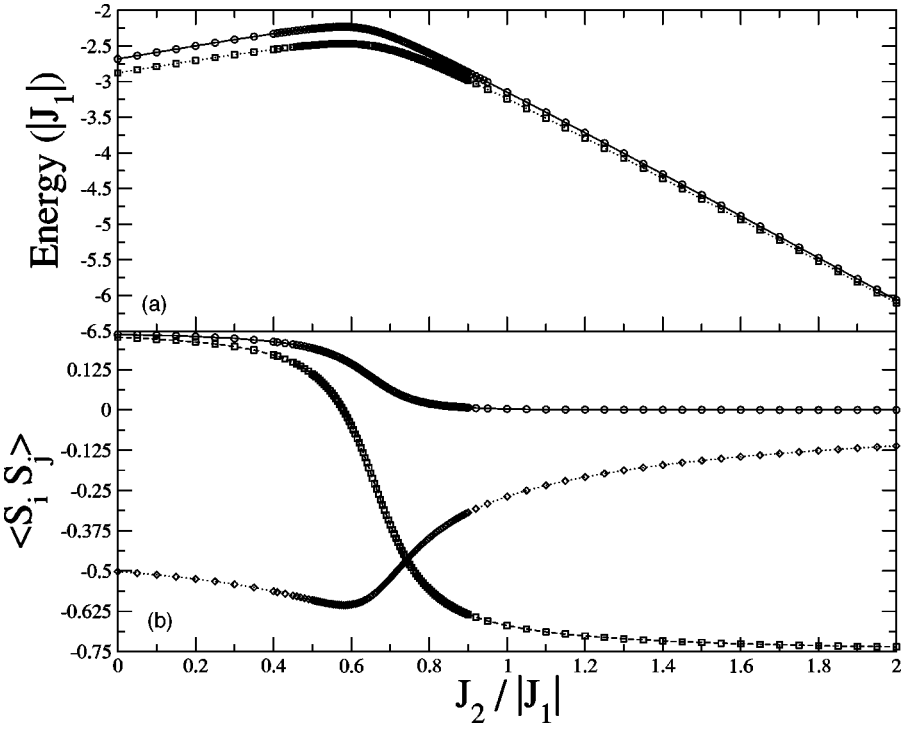

FIG. 5. Energy and nearest and next nearest neighbor correlation functions of the ground state for $s_i = 1/2$ and a $2\times2\times2$ cluster as a function of $J_2/|J_1|$. [(a) Top] $J_3/|J_1| = 0.4$ (○) and $J_3/|J_1| = 0.5$ (□). [(b) Bottom] correlation function for bond J_1 (○), for bond J_2 (□), and for bond J_3 (◇). The lines are guides for the eye.

in the 8-site cluster. It is expected that the results for the $s_i = 7/2$ case will be similar and the point where correlation functions change will be closer to 1, compared with the 8-site case. This result agrees with linear spin wave theory, where quantum fluctuations have a small effect on the classical solution.

When $s_i = 1/2$ full diagonalization is possible for systems of 18 sites; $3\times3\times2$ cluster Hamiltonians were diagonalized. The specific heat of the cluster is plotted in Fig. 7(a) as a function of temperature for several values of $J_2/|J_1|$. There is a shoulder at low energy which disappears for $J_2/|J_1| > 0.7$, again indicating a change in the nature of the ground state. At the same time, the main peak is pushed toward lower temperature and its value decreases. The magnetic susceptibility as a function of temperature is shown in Fig. 7(b). The shoulder found for lower $J_2/|J_1|$ values disap-

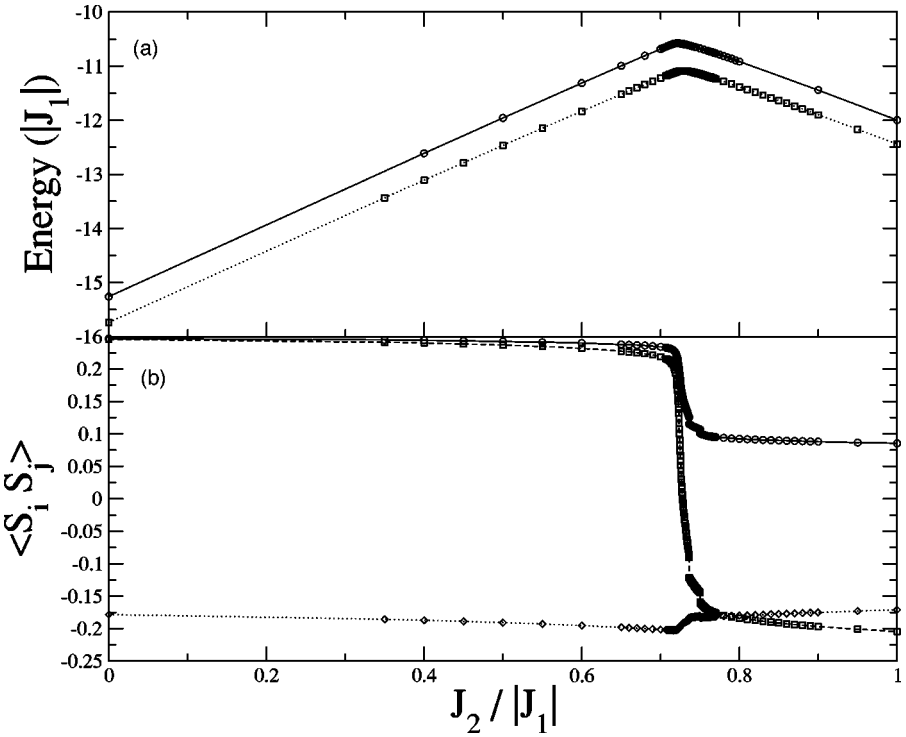

FIG. 6. Energy and nearest and next nearest neighbor correlation functions of the ground state for $s_i = \frac{1}{2}$ and a $3\times3\times3$ cluster as a function of $J_2/|J_1|$. [(a) Top] $J_3/|J_1| = 0.4$ (○) and $J_3/|J_1| = 0.5$ (□). [(b) Bottom] correlation function for bond J_1 (○), for bond J_2 (□), and for bond J_3 (◇). The lines are guides for the eye.

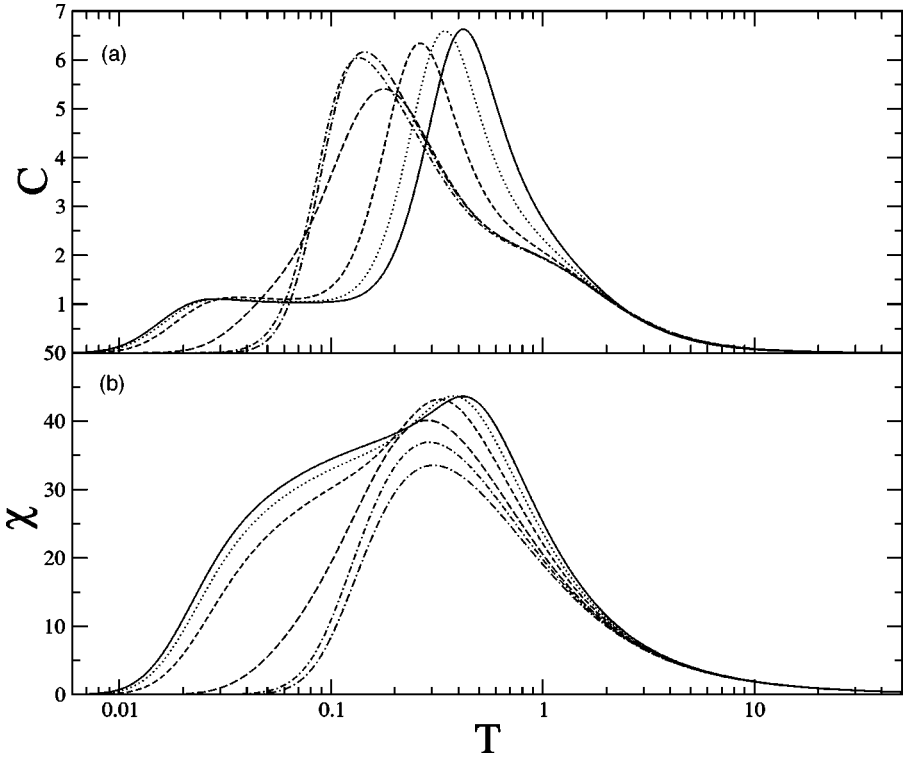

FIG. 7. Specific heat [(a) top] and susceptibility [(b) bottom] as function of temperature for $J_3/|J_1|=0.5$. solid line: $J_2/|J_1|=0.4$, dotted line: $J_2/|J_1|=0.5$, dashed line: $J_2/|J_1|=0.6$, long-dashed line: $J_2/|J_1|=0.7$, dot-dashed line: $J_2/|J_1|=0.75$, dot-long dashed line: $J_2/|J_1|=0.8$.

pears for higher values and the peak position shifts to lower temperature, signifying again a qualitative change as the frustrating interaction gets stronger.

V. CONCLUSIONS

A Heisenberg model with FM nearest neighbor interactions J_1 and AF next nearest and interplanar interactions J_2 and J_3 has been studied as a prototype for the magnetic behavior of polarons forming in the half-doped lanthanum manganite $La_{0.5}Ca_{0.5}MnO_3$.[5] The polarons are spin 7/2 objects formed by two Mn and an O ion. At the classical level the ground state is of the A-type for $J_2/|J_1|\leqslant 0.5$, while for higher J_2 it is a spin spiral. When $J_2/|J_1|>0.5$, there is a spiral in the *xy* plane with every other pair of spins parallel in zig-zag chains, and an angle $q=\arccos(-J_1/2J_2)$ between neighboring spins. For $J_2/|J_1|\to\infty$ the spiral becomes the orthogonal state described by Efremov *et al.* in Ref. 6, where polaron moments are perpendicular to each other along the zig-zag chains and antiparallel along the direction of J_2. The effect of quantum fluctuations on spin wave theory is small due to the large magnitude of the spins, $s_i=7/2$. Hence the magnetization per site is not significantly changed from its classical value. Diagonalization of finite clusters also shows that quantum fluctuations do not significantly alter the classical solution, and the ratio $J_2/|J_1|$ for which there is a transition from FM order in the planes to one where spins are coupled antiferromagnetically via the J_2 bond is close to its value at the classical level.

The calculations in this paper show that the magnetic structure of Zener polarons in $La_{0.5}Ca_{0.5}MnO_3$ is subtly dependent on the ratio $J_2/|J_1|$. The value from *ab initio* calculations was found to be 0.38,[5] however UHF calculations underestimate the value of AF couplings, and recent calculations of real space structure tend to favor a ratio close to 0.5 with a CE-type magnetic ground state.[7] Thus the physically relevant parameter space of the Hamiltonian [Eq. (1)] has $J_2/|J_1|\sim 0.5$, where for $J_2/|J_1|>0.5$ the magnetic structure is non-bipartite and depends on the exact value of $J_2/|J_1|$. Similar conclusions have been drawn by Efremov *et al.* in Ref. 6. In that paper the authors have found that around half-doping magnetic order depends sensitively on the extent of doping *x*, and the orthogonal state is the ground state for a part of the phase diagram, while a state which is a superposition of the conventional CE-type order and the orthogonal phase is lowest in energy for different combinations of parameters. The angle between neighboring spins is $2\pi/3$ in that phase. In our model the angle between spins linked via the J_2 bond and belonging to different zig-zag chains is $2\pi/3$ when $J_2/|J_1|=1$, while the angle between nearest neighbors is $\pi/3$ in that case. This phase is also weakly renormalized by quantum fluctuations. Therefore the Hamiltonian [Eq. (1)] predicts phases which differ from the conventional CE-type order.

Diagonalization of small clusters with cubic symmetry also showed that there is a change in the character of the ground state as a function of $J_2/|J_1|$. For small ratios spins are ferromagnetically ordered within planes, while for higher values the next-nearest neighbor AF interaction dominates. As was the case with linear spin wave theory, the diagonalizations show that the classical results are not significantly altered by quantum fluctuations. A spin magnitude of $s_i=1/2$ was also considered to study finite size effects, and the transition from the 8- to the 27-site cluster showed that the ratio where the character of the ground state changes comes closer to the classical value. Results from larger clusters would be needed to firmly establish this point, however memory requirements prohibit diagonalizations of larger cu-

bic clusters. The role of the AF interaction J_2 was also evident in full diagonalizations of the model for systems of 18 sites with $s_i=1/2$. Specific heat and magnetic susceptibility data were calculated, and the graphs change qualitatively as a function of $J_2/|J_1|$, showing again the role of the diagonal AF interaction in the development of AF intraplane correlations.

The spin wave dispersion was calculated for the material $Nd_{0.45}Sr_{0.55}MnO_3$ in Ref. 29, and it was fitted with a Heisenberg model with FM nearest neighbor interactions in the planes and AF interactions between planes. There was also an anisotropy term. The relative strength of the AF with respect to the FM interaction was found to be 0.620, which is in agreement with the values in Ref. 5. The anisotropic interaction was relatively small.

Spin wave calculations by Ventura and Alascio[15] were performed for a 16 spin per unit cell Heisenberg Hamiltonian with FM interactions within zig-zag chains and AF interactions between chains. Calculations were reported for a CO state with spin magnitudes in the ratio 1.3:1 and all FM interaction strengths the same and also for a dimer (Zener polaron) state where all spin magnitudes were the same, but FM interactions within dimers were much stronger than inter-dimer FM interactions. As noted above, the main differences in these models is that there is one spin per Zener polaron and chain-chain interactions are frustrated in our model, whereas in Ref. 15 each Mn ion is represented by a spin and chain-chain interactions are not frustrated. Our model does not contain the optical branches reported by Ventura and Alascio, which arise from intra-dimer spin excitations. The main difference in predictions is expected for in-plane dispersion along AF inter-chain bonds. These are frustrated in our model and lead to a spin spiral state when $|J_2|/J_1>0.5$, with a wave vector determined by the spin wave zero mode along the (k,k,π) direction (top panel in Fig. 3). In Ref. 15 in-plane AF inter-chain bonds are not frustrated and no zero mode is expected; dispersion along that direction is not shown in Ref. 15.

ACKNOWLEDGMENTS

The authors wish to acknowledge discussions with R. Kenna. Calculations were carried out at the Trinity Centre for High Performance Computing. Computing facilities were provided by the Irish Higher Education Authority under the PRTLI-III program IITAC-II. N.P.K. was supported by a Marie Curie Fellowship of the European Community program Development Host Fellowship under contract number HPMD-CT-2000-00048.

*Present address: Leoforos Syggroy 360, Kallithea 176 74, Athens, Hellas.

[1] J. B. Goodenough, Phys. Rev. **100**, 564 (1955).
[2] E. Dagotto, *Nanoscale Phase Separation and Colossal Magnetoresistance* (Springer, Berlin, 2002).
[3] P. G. Radaelli, D. E. Cox, M. Marezio, and S.-W. Cheong, Phys. Rev. B **55**, 3015 (1997).
[4] A. Daoud-Aladine, J. Rodriguez-Carvajal, L. Pinsard-Gaudart, M. T. Fernandez-Diaz, and A. Revcolevschi, Phys. Rev. Lett. **89**, 097205 (2002).
[5] G. Zheng and C. H. Patterson, Phys. Rev. B **67**, 220404(R) (2003).
[6] D. V. Efremov, J. van den Brink, and D. I. Khomskii, cond-mat/0306651.
[7] C. H. Patterson (unpublished).
[8] F. Rivadulla, E. Winkler, J.-S. Zhou, and J. Goodenough, Phys. Rev. B **66**, 174432 (2002).
[9] M. Nicastro and C. H. Patterson, Phys. Rev. B **65**, 205111 (2002).
[10] R. Kajimoto, H. Yoshizawa, Y. Tomioka, and Y. Tokura, Phys. Rev. B **66**, 180402 (2002).
[11] E. O. Wollan and W. C. Koehler, Phys. Rev. **100**, 545 (1955).
[12] A. E. Trumper, Phys. Rev. B **60**, 2987 (1999).
[13] W. Zheng, R. H. McKenzie, and R. R. P. Singh, Phys. Rev. B **59**, 14 367 (1999).
[14] N. Suaud and M.-B. Lepetit, Phys. Rev. B **62**, 402 (2000).
[15] C. I. Ventura and B. Alascio, Phys. Rev. B **68**, 020404 (2003).
[16] J. Villain, J. Phys. Chem. Solids **11**, 303 (1959).
[17] A. Yoshimori, J. Phys. Soc. Jpn. **14**, 807 (1959).
[18] T. Holstein and H. Primakoff, Phys. Rev. **58**, 1098 (1940).
[19] N. N. Bogoliubov, J. Phys. (USSR) **9**, 23 (1947).
[20] N. N. Bogoliubov, Nuovo Cimento **7**, 794 (1958).
[21] J. Merino, R. McKenzie, J. B. Marston, and C. H. Chung, J. Phys.: Condens. Matter **11**, 2965 (1999).
[22] N. D. Mermin and H. Wagner, Phys. Rev. Lett. **17**, 1133 (1966).
[23] B. Bernu, P. Lecheminant, C. Lhuillier, and L. Pierre, Phys. Rev. B **50**, 10 048 (1994).
[24] W. Florek and S. Bucikiewicz, Phys. Rev. B **66**, 02441 (2002).
[25] O. Waldmann, Phys. Rev. B **61**, 6138 (2000).
[26] R. Lehoucq, K. Maschhoff, D. Sorensen, and C. Yang, www.caam.rice.edu/software/ARPACK/
[27] S. Shaw, www-heller.harvard.edu/shaw/programs/lapack.html
[28] S. L. Altmann and P. Herzig, *Point-Group Theory Tables* (Oxford University Press, New York, 1994).
[29] H. Yoshizawa, H. Kawano, J. A. Fernandez-Baca, H. Kuwahara, and Y. Tokura, Phys. Rev. B **58**, R571 (1998).